drones

MDPI

Article

Assessing the Severity of Verticillium Wilt in Cotton Fields and Constructing Pesticide Application Prescription Maps Using Unmanned Aerial Vehicle (UAV) Multispectral Images

Xiaojuan Li [1,*], Zhi Liang [1], Guang Yang [1], Tao Lin [2] and Bo Liu [1]

[1] School of Mechanical Engineering, Xinjiang University, Urumqi 830017, China; 107552201439@stu.xju.edu.cn (Z.L.)
[2] Institute of Cash Crops, Xinjiang Academy of Agricultural Sciences, Urumqi 830091, China
* Correspondence: xjli@xju.edu.cn

Abstract: Cotton Verticillium wilt is a common fungal disease during the growth of cotton, leading to the yellowing of leaves, stem dryness, and root rot, severely affecting the yield and quality of cotton. Current monitoring methods for Verticillium wilt mainly rely on manual inspection and field investigation, which are inefficient and costly, and the methods of applying pesticides in cotton fields are singular, with issues of low pesticide efficiency and uneven application. This study aims to combine UAV remote sensing monitoring of cotton Verticillium wilt with the precision spraying characteristics of agricultural drones, to provide a methodological reference for monitoring and precision application of pesticides for cotton diseases. Taking the cotton fields of Shihezi City, Xinjiang as the research subject, high-resolution multispectral images were collected using drones. Simultaneously, 150 sets of field samples with varying degrees of Verticillium wilt were collected through ground data collection, utilizing data analysis methods such as partial least squares regression (PLSR) and neural network models; additionally, a cotton Verticillium wilt monitoring model based on drone remote sensing images was constructed. The results showed that the estimation accuracy R^2 of the PLSR and BP neural network models based on EVI, RENDVI, SAVI, MSAVI, and RDVI vegetation indices were 0.778 and 0.817, respectively, with $RMSE$ of 0.126 and 0.117, respectively. Based on this, an analysis of the condition of the areas to be treated was performed, combining the operational parameters of agricultural drones, resulting in a prescription map for spraying against cotton Verticillium wilt.

Keywords: cotton Verticillium wilt; unmanned aerial vehicle (UAV) remote sensing; monitoring model; precision spraying; prescription map

check for updates

Citation: Li, X.; Liang, Z.; Yang, G.; Lin, T.; Liu, B. Assessing the Severity of Verticillium Wilt in Cotton Fields and Constructing Pesticide Application Prescription Maps Using Unmanned Aerial Vehicle (UAV) Multispectral Images. *Drones* **2024**, *8*, 176. https://doi.org/10.3390/drones8050176

Academic Editor: Yangquan Chen

Received: 26 March 2024
Revised: 25 April 2024
Accepted: 29 April 2024
Published: 30 April 2024

1. Introduction

Cotton is one of the world's important economic crops, its yield and quality are of great significance to both farmers and the national economy [1]. However, the production of cotton is often threatened by various diseases and pests, among which cotton Verticillium wilt is a serious disease. Cotton Verticillium wilt is a vascular disease caused by a soil-borne pathogenic fungus (*Verticillium dahliae*), this disease occurs easily under hot and humid climate conditions, leading to the yellowing of leaves, rotting of stems and roots, necrosis, and eventually death of the plant, severely affecting the yield and quality of cotton [2,3].

Currently, the monitoring method for Fusarium wilt mainly relies on field manual inspection, primarily on the identification of Fusarium wilt characteristics, such as yellowing, withering, fading or changing color of leaves, lesions, fuzzy edges, etc., and assesses the severity of Fusarium wilt based on the size, color, and distribution of lesions on leaves, usually combining some qualitative or quantitative assessment indicators, such as the proportion of lesion area, the number of infected plants, etc., to evaluate the impact of diseases in cotton fields [4,5]. Upon detecting Verticillium wilt, it is common to employ agricultural drones to carry out multiple rounds of extensive spraying, using anti-Verticillium agents and fungicides to curb the further spread of the disease within the affected areas and to prevent healthy areas from being invaded by the pathogen [6,7]. However, outbreaks of Verticillium wilt often occur in a patchy pattern, and extensive spraying of pesticides can lead to uneven application, residue, and pollution issues. High concentrations of the solution can cause toxic effects such as leaf burn, chlorosis, stunted growth, and flower wilting, leading to reduced cotton yield or quality [8,9]. Moreover, the long-term extensive use of the same or similar types of pesticides is very likely to induce resistance to pests and diseases, reducing the efficacy of treatments and making it difficult to control these issues effectively [10]. If disease and healthy areas within medium and small-scale cotton fields can be accurately identified, and precise area segmentation and graded treatment can be implemented based on the severity of the disease, along with regular monitoring of disease progression, it is possible to significantly reduce the widespread residue issues caused by treating Verticillium wilt. Therefore, improving the monitoring methods for Verticillium wilt and achieving precise application of pesticides in cotton fields is of great importance for increasing cotton yield and quality, reducing pesticide use, preventing resistance issues, and promoting sustainable agricultural development.

Existing methods for monitoring cotton field diseases are inefficient, inaccurate, and costly, and are only suitable for medium and small-scale cotton fields. With the rapid development of low-altitude remote sensing technology using drones, researchers have conducted cotton field disease monitoring using drone remote sensing diagnosis [11]. Xavier et al. used three spectral bands (near infrared (NIR), red, and green) as input features and employed supported vector machine (SVM), multinomial logistic regression (MLR), and random forest (RF) for machine learning classification of cotton field remote sensing images, finding that SVM outperforms all other ML models in detecting cotton leaf wilt disease [12]. Wang et al. proposed an automated method combining k-means segmentation and morphological opening and closing, achieving automatic classification of cotton root rot (CRR) in high-resolution drone remote sensing imagery [13]. Abdalla et al. proposed a method combining time series analysis and convolutional neural networks-bidirectional long-short term memory (CNN-BiLSTM) to overcome the challenges of spatiotemporal variation and domain transfer in estimating plant diseases using UAV system images. They achieved an overall classification accuracy of 89.7% on a one-year dataset and demonstrated a generalization capability of 72.7% in cross-temporal and spatial disease severity classification, effectively promoting the development of field crop disease assessment [14]. Wang et al. used drones to obtain multispectral images, capturing split-frame canopy images of cotton and converting them into the Lab* color space for training or validation samples. By processing and combining two types of images, they established a model for the inversion of cotton wilt disease infection and validated it with ground-based frame photos, providing an effective monitoring method for cotton wilt [15]. Lu et al. addressed the issue of inefficient traditional manual operations in identifying cotton Fusarium wilt and proposed a new method that combines spectral and image features. A classification model was constructed by collecting hyperspectral images and applying various preprocessing and feature extraction methods. The savitzky golay smoothing-mean normalization-successive projections algorithm-feature fusion-back propagation neural network (SG-MN-SPA-FF-BPNN) model with fused spectral and image features achieved the best performance of 98.99%, providing a theoretical basis and method for monitoring cotton Fusarium wilt [16].

Precision pesticide spraying refers to the use of navigation positioning systems, geographic information technology, or real-time sensor technology to generate spray prescription maps based on different information about crops or pests and diseases, and converting them into precise values for pesticide application. By adjusting the spray volume, speed, or other parameters of the nozzle, targeted and differentiated pesticide spraying operations can be achieved [17,18]. Precision spraying can reduce the amount of pesticides used and improve their utilization rate, and it has been widely applied in the field of crops [19]. For example, Campos et al. addressed the problem of time-consuming and inaccurate manual measurements of vineyard canopy characteristics and proposed a characterization method based on UAV and satellite images. The relationship between manual and remote feature data was analyzed through regression models, and clustering was performed based on vine vigor levels. This achieved rapid and reliable estimation of canopy characteristics and provided a theoretical basis for variable spraying in vineyards [20]. Yu et al. extracted five high-spectral variables of rice within the 450–950 nm range and constructed a rice nitrogen content inversion model based on the whale optimization algorithm and extreme learning machine (WOA-ELM), realizing the diagnosis of rice nitrogen requirements through drone hyperspectral remote sensing during the fertilization window of the cultivation period. The results provide data and model bases for the precise variable fertilizer tracking of agricultural drones during the tillering stage of cold-water rice [21]. Rudd et al. addressed the issue of excessive application of defoliant in cotton-growing areas by including cotton plant height and normalized difference vegetation index (NDVI) as primary factors for variable spraying. The differences within the cotton canopy were expressed by manually setting factor weights, achieving variable spraying of defoliant [22]. Li et al. trained a U-Net with a crop dataset for crop segmentation and utilized color indices and the Otsu thresholding algorithm for vegetation segmentation. Then, by removing the crop area from the vegetation segmentation results, they achieved weed segmentation and created a weed dataset, which was used to train an improved pyramid spatial pooling (PSP) network for weed segmentation. The ratio of weed pixels to the total number of pixels in a regionally segmented image was calculated to measure weed density. Finally, based on the weed density threshold, prescription maps representing different treatment intensities were generated [23]. These studies, by leveraging crop growth and plant characteristics to achieve sensor-based variable prescription maps for pesticide application, highlight the use of diverse information about crops as a hot topic in precision agriculture research.

In summary, cotton Fusarium wilt monitoring faces multiple challenges. Currently, research on disease and pest control mainly focuses on cotton field disease detection. The accuracy of traditional machine learning classification methods in cotton Fusarium wilt monitoring is affected by the quality of the dataset. Due to the gradual leaf shedding in the late stage of cotton Fusarium wilt, classifiers tend to misjudge the severity of the disease, leading to a decrease in monitoring effectiveness. As the infection severity of Fusarium wilt increases, plants lose water and chlorophyll content decreases, making the crown disease characteristics more pronounced, thereby enhancing the sensitivity of vegetation indices to disease responses. Therefore, the study combined vegetation indices strongly correlated with Fusarium wilt to construct PLSR and BP neural network monitoring models. Furthermore, existing cotton field disease detection models are difficult to directly guide cotton field management, lacking research combining disease severity diagnosis with precise spraying of plant protection equipment. Therefore, this study combines the drone remote sensing diagnosis of cotton Verticillium wilt with the precision spraying features of agricultural drones, using drone multispectral imagery to establish a monitoring map for cotton Verticillium wilt disease condition, and on this basis, combining agricultural drone operation parameters to analyze the condition of the areas to be treated with pesticides. This approach creates a prescription map for applying pesticides to cotton fields affected by Verticillium wilt, offering a methodological reference for cotton disease monitoring and precision pesticide application.

2. Materials and Methods

2.1. Study Area

The experimental site is located in the 142nd Regiment, Seventeenth Company, Shihezi City, Xinjiang Uyghur Autonomous Region, China (longitude 85.33–85.34, latitude 44.28–44.29) (see Figure 1). This area is situated in a temperate continental arid and semi-arid climate zone, with an average annual temperature of 8.1 °C, average annual sunshine duration of about 2700 h, scarce cloudiness, annual rainfall of 225 mm, annual evaporation of 1250 mm, and a significant temperature difference between day and night. Agricultural production is entirely dependent on irrigation. The soil texture in the experimental area is sandy loam, with a field water holding capacity of 28.92%, medium soil fertility, and a soil pH value of 7.33. The cotton variety tested is Xinluzao 77, planted on 26 April 2023, with a planting density of 18,000 plants per hectare. The area of the experimental field is 8250 square meters.

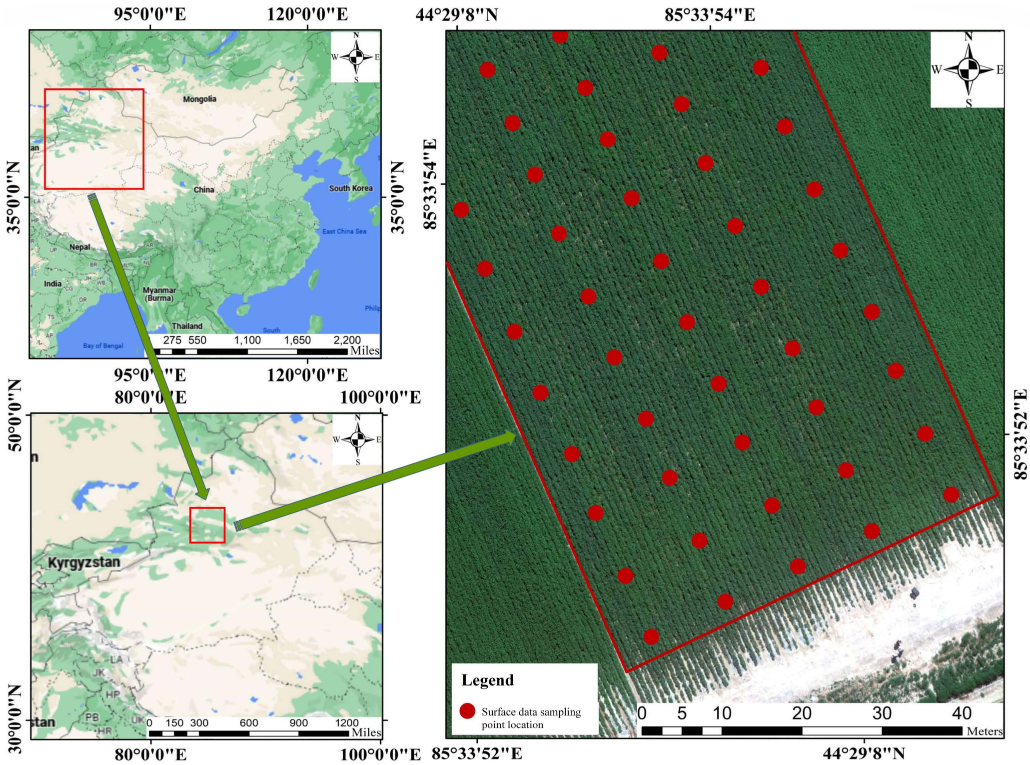

Figure 1. Study area and spatial distribution of the experimental site in cotton field of Company 17, 142 Mission Field, Shihezi City, Xinjiang.

2.2. Data Acquisition

2.2.1. Acquisition of Multispectral Images by Unmanned Aerial Vehicle

The study used the M300 RTK multirotor drone (DJI, Shenzhen, China) (see Figure 2a) and the RedEdge-MX-Dual airborne multispectral imager (MicaSense, Seattle, WA, USA) (see Figure 2b) for data collection. The M300 RTK supports the Real-Time Kinematic (RTK) positioning system, which utilizes ground reference station data for real-time correction, providing higher positioning accuracy. It can achieve positioning accuracy of 1 cm ± 1 ppm in the horizontal direction and 1.5 cm ± 1 ppm in the vertical direction, enabling the M300 RTK to meet higher precision requirements in fields such as mapping and precision navigation. The RedEdge-MX-Dual has a ground sampling distance (GSD) of 8 cm at a hover altitude of 120 m. The camera captures ten channels within the 400–900 nm spectral range, including coastal blue, blue, green, red, red edge, and near-infrared.

UAV images of the study area were collected between 11:00–12:00 on 18 July 2023. At this time, cotton was in the boll stage, during the peak period of cotton Verticillium wilt, under clear weather conditions, with a wind force of level 1, and a temperature of about 38 °C. The drone's flying altitude was set to 50 m, with a GSD of 3.47 cm/pixel, a forward overlap of 80%, and a side overlap of 80%. A downlink light sensor (DLS) was used to correct for global illumination changes during the flight, including variations caused by cloud cover (see Figure 2c), and a set of correction images was taken before and after the flight. The camera was positioned 1 m above a diffuse reflectance reference board, with a reflectance of 50%, located in the middle of the screen (see Figure 2d).

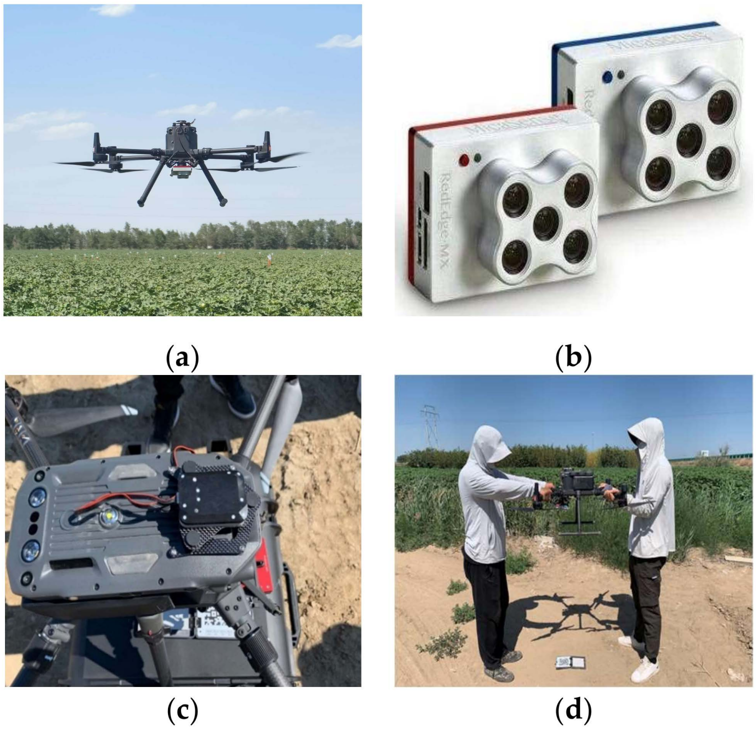

Figure 2. Multispectral image acquisition equipment: (**a**) M300 RTK multicopter, (**b**) RedEdge-MX-Dual airborne multispectral imager, (**c**) DLS optical sensor, (**d**) calibrated reflectance panel (CRP).

2.2.2. Classification of Verticillium Wilt Disease Severity in the Field

Due to the continuous invasion and cumulative effects of Verticillium wilt, the health status of cotton will gradually deteriorate, manifesting as continuous changes in leaf symptoms, with leaf symptoms at different infection levels shown in Figure 3. In this study, based on the disease index (DI) of the cotton Verticillium wilt test population, the severity of canopy disease was divided into five levels [24] (see Table 1). To ensure randomness and uniformity of sampling points, ground monitoring points were arranged in a grid pattern. A manual 50 cm $\times$ 50 cm auxiliary frame was made and placed at the cotton canopy of the monitoring points (Figure 4a). According to the cotton Verticillium wilt detection and reporting technical standard NYT 3700-2020, the severity of cotton Verticillium wilt was statistically analyzed, calculating the disease index at each monitoring point and classifying the severity of the disease. Simultaneously, the latitude and longitude of the center of the frame were measured using handheld RTK global positioning system (GPS) equipment (Figure 4b), ultimately obtaining 150 ground-truth data points of Verticillium wilt with various severities and geographic coordinates, the distribution of samples is shown in Table 2.

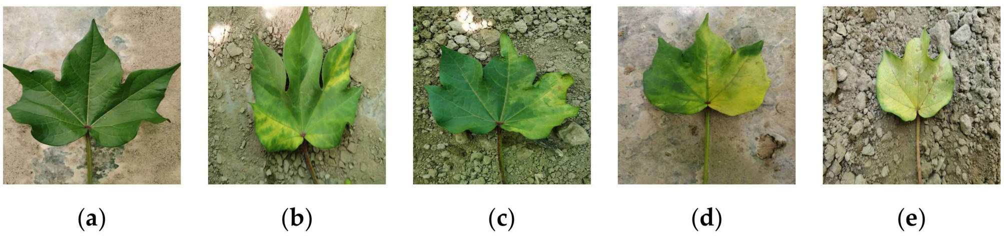

Figure 3. Leaf symptoms of Verticillium wilt at different infection levels: (**a**) healthy, (**b**) slight infection, (**c**) mild infection, (**d**) moderate infection, (**e**) severe infection.

Table 1. Cotton Verticillium wilt disease severity grading criteria.

Disease Severity	Disease Index (DI)	Disease Division Standard
b0 (Health)	0	Healthy plants, no diseased leaves.
b1 (Slight)	$0 < \text{DI} \leq 25\%$	Symptoms are visible on less than 1/4 of the leaves, with yellowish or yellow irregular lesions between the main veins of the leaf.
b2 (Moderate)	$25\% < \text{DI} \leq 50\%$	1/4 to 1/2 of the leaves show symptoms, most of the spots are yellow or yellow–brown, the edge of the leaf blade is slightly curled withered.
b3 (Serious)	$50\% < \text{DI} \leq 75\%$	1/2 to 3/4 of the leaves show disease, with a few leaves falling off.
b4 (Critical)	$75\% < \text{DI} \leq 100\%$	More than 3/4 leaf disease, mostly brown spots, cotton plant leaf shedding for light pole, or even death.

(**a**) (**b**)

Figure 4. Ground survey of cotton Verticillium wilt disease severity: (**a**) auxiliary frame, (**b**) RTK GPS measuring equipment.

Table 2. The distribution of samples across different disease severity levels.

Disease Severity	B0	B1	B2	B3	B4
Number of samples	11	21	20	68	30
Proportion	7.33%	14%	13.34%	45.33%	20%

The disease index (DI, %) was derived using the following method, based on the cotton Verticillium wilt disease severity grading standard:

$$\text{DI} = \frac{\sum(X \cdot f) \cdot 100}{n \cdot \sum f} \tag{1}$$

where X denotes the number of disease severity levels, n is the number of greatest illness levels, and f is the number of plants at each level.

2.2.3. Unmanned Aerial Vehicle (UAV) Image Data Preprocessing

Drone images were pre-processed using Agisoft Metashape Professional (v2.0.1), including steps such as initialization, aerial triangulation, radiometric correction, feature point matching (edge joining, color adjustment, mosaicking, and cropping), spectral vegetation index (SVI) calculation, and the generation of RGB (red, green, blue) images and vegetation index images. To enhance the geometric accuracy of drone imagery, aerial triangulation processing was conducted using ground targets as image control points. Simultaneously, to ensure the calibration accuracy of drone imagery, a radiometric correction method was introduced. This involves calibrating drone images using two diffuse reflectance reference panels (one captured before flight, and the other captured after flight), ultimately generating high-precision multispectral drone digital orthophoto imagery (DOM). To obtain the distribution of vegetation indices in remote sensing image data, square regions of interest (ROIs) of equal size are drawn around ground-truthed points using the region of interest (ROI) tool in ENVI (Environment for Visualizing Images), centered at the latitude and longitude of the collected ground points. These ROIs are used to mark the ground survey area, and spectral indices are calculated for all ROIs using the band calculation tool in ENVI. The study selected ten vegetation indices extensively used in cotton disease monitoring (see Table 3), such as the ratio vegetation index (RDVI), soil-adjusted vegetation index (SAVI), enhanced vegetation index (EVI), modified soil-adjusted vegetation index (MSAVI), and red-edge normalized difference vegetation index (RENDVI), among others.

Table 3. Vegetation index calculation formula.

Vegetation Index	Formula	References
Ratio vegetation index (RVI)	$\frac{NIR}{R}$	[25]
Renormalized difference Vegetation index (RDVI)	$\frac{NIR-R}{\sqrt{NIR+R}}$	[26]
Green normalized difference vegetation index (GNDVI)	$\frac{NIR-G}{NIR+G}$	[27]
Red edge normalized difference vegetation index (RENDVI)	$\frac{NIR-RE}{NIR+RE}$	[28]
Difference vegetation index (DVI)	$NIR - R$	[29]
Soil adjusted vegetation index (SAVI)	$\frac{(NIR-R)*(1+L)}{(NIR+R+L)}$	[30]
Optimized soil adjusted vegetation index (OSAVI)	$\frac{1.16*(NIR-R)}{NIR+R+0.16}$	[31]
Modified soil adjusted vegetation index (MSAVI)	$2*(NIR+1)-\frac{\sqrt{(2*NIR+1)^2-8(NIR-R)}}{2}$	[32]
Enhanced vegetation index(EVI)	$\frac{2.5*(NIR-R)}{(NIR+6*R-7.5*B+1)}$	[33]
Normalized difference water index (NDWI)	$\frac{G-NIR}{G+NIR}$	[34]

Note: B represents the blue band, G represents the green band, R represents the red band, RE represents the red edge band, NIR represents the near-infrared band, and L is the soil adjustment parameter, ranging from zero to one.

2.2.4. Setting Parameters for Agricultural Drone Operation

Prescription maps represent dosage levels, system response data, and the overlay of geographic information layers. Single spatial distribution data cannot meet the operational requirements of agricultural equipment. With the advancement of drone technology, unmanned aerial spraying systems have rapidly developed and are widely used in cotton field spraying. They possess rapid and accurate spraying capabilities, as well as high operational flexibility and efficiency [35]. Drones can autonomously fly and perform automated operations along preset paths and parameters, reducing labor costs and environmental pollution risks. However, current cotton field drone spraying mostly adopts quantitative spraying, lacking operational guidance information combined with agricultural monitoring. Therefore, the construction of prescription maps is crucial for achieving precise drone spraying. Taking the DJI T16 agricultural drone as an example, this study analyzes the disease situation in cotton fields based on drone operational parameters. The drone spraying width is 4–6.5 m, with a maximum load of 15.1 L, nozzle model XR11001VS, and flight mode in autonomous control mode. The drone operational conditions such as wind speed, temperature, and humidity must comply with the relevant provisions of GB/T 25415 and NY/T 1533. In addition, the quality requirement for drone operations is that the uniformity of droplet distribution should be less than 50%, and the requirements for agricultural drone operational parameters (Table 4) and the calculation of spraying rate per unit time refer to the Technical Guidelines for Agricultural Drone Cotton Field Spraying T/CCPIA 057—2020.

Table 4. Parameter requirements for plant protection drone operations on cotton.

Volume of Liquid Applied L/hm^2	Altitude m	Flight Speed m/s
1–1.5	1.5–4	3.5–5.5

The amount of pesticide applied per unit of time was calculated based on the parameters of plant protection drone operation with the following formula:

$$Q = \frac{V \times q \times D \times 60}{10,000} \tag{2}$$

where Q is the total flow rate of the nozzle; V is the flight speed; q is the amount of liquid applied; and D is the spray width.

2.3. Data Analysis and Evaluation

This study first analyzed the spectral characteristics of different disease levels in the cotton canopy, combined with their sensitivity to spectral features, and conducted a correlation analysis between ten sets of spectral index values in the target area of remote sensing images and ground-truthed data of Fusarium wilt disease severity to select suitable spectral indices. Secondly, it identified vegetation indices highly correlated with the severity of Fusarium wilt disease, and used partial least squares regression models and BP neural networks with ground-truthed data as target values. The vegetation indices with high correlations in the remote sensing data were used as multivariate variables for modeling, to establish a predictive model of Fusarium wilt disease severity. Finally, the accuracy of the established model was evaluated by combining ground-truthed data for the precision assessment of its predictive ability. The study obtained 150 ground data samples of Verticillium wilt severity. Since collecting empirical data for the study required significant labor, and although as many measurements as possible were taken to ensure model training accuracy, the dataset remained a small sample set. Therefore, the data were divided into training and testing sets in an 8:2 ratio, with 80% of the samples (120 samples) selected randomly as the training set and 20% of the samples (30 samples) used as the test set.

2.3.1. Partial Least Squares Regression

Partial least squares regression (PLSR) is a technique that simultaneously performs dimensionality reduction and regression analysis. It predicts one or more response variables by mapping high-dimensional input features to a lower-dimensional space [36]. PLSR integrates the advantages of principal component analysis (PCA) and multiple linear regression (MLR). By constructing latent variables that maximize the correlation between predictor variables and response variables, it effectively addresses the problem of high correlation or multicollinearity between variables [37]. In the regression process, the number of selected predictor variables is crucial for the model's performance. Too many variables may lead to overfitting, while too few may fail to capture enough information. In PLSR analysis, the variable importance in projection (VIP) value is an important indicator of the explanatory power of predictor variables for response variables. It is calculated by considering the influence of each predictor variable on each latent variable comprehensively. A higher VIP value indicates a greater contribution of the corresponding predictor variable to explaining the variance of the response variable [38]. Its calculation formula is as follows:

$$\sqrt{n\frac{\sum_{j=1}^{a} b_j^2 t_j^T t_j \left(\frac{w_{kj}}{||w_j||}\right)^2}{\sum_{j=1}^{a} b_j^2 t_j^T t_j}} \tag{3}$$

where b is the regression coefficient, w_j is the weight vector, and t_j is the score vector for the k^{th} element.

This study implemented the partial least squares regression (PLSR) algorithm in the Python 3.7 environment using the partial least squares regression function from the Scikit-Learn (1.0.2) package. The selection of model predictors was based on the VIP values. By mapping the original data to the latent variable space, redundant information in the data was reduced, thereby enhancing the predictive performance and interpretability of the model [39]. Additionally, the model was built by maximizing the covariance between predictor and response variables, aiming to improve the predictive ability and robustness of the model under small sample data.

2.3.2. Backpropagation Neural Network

Backpropagation neural network (BP neural network) is a perceptual machine-based neural network model that is frequently employed in the solution of classification and regression issues [40]. The backpropagation algorithm is used to train the BP neural network, which contains three types of neural network layers: a input layer, a hidden layer, and an output layer. The input layer of a BP neural network accepts input data, the hidden layer analyzes the information and extracts the features using many neurons, and the output layer provides the final prediction result. By modifying the network's weights and biases, the BP neural network may learn and adapt the model to minimize the difference between anticipated and actual values. BP neural networks typically feature more than one hidden layer, with each hidden layer containing a varied number of neurons. BP neural networks may extract higher-order feature information by increasing the number of hidden layers and the size of neurons, which increases the model's performance and expressiveness [41].

This study implemented the construction of a BP neural network using the Pytorch (1.7.1) deep learning library in the Python 3.7 environment. Rectified linear unit (ReLU) was selected as the activation function in the network model, the mean squared error was used as the optimization function, the mean squared error was chosen as the loss function, and the model iteration was set to 100 times.

2.3.3. Model Evaluation Indicators

The indicators for evaluating the prediction model in this study were the coefficient of determination (R^2) and the root mean square error ($RMSE$). The $RMSE$ is the average error between the prediction and actual condition index results. The model computations yielded the predicted results, and the actual results were compared to the manual ground truth data in Section 2.2.2. The greater the R^2 and the lower the $RMSE$ of the prediction and validation models, the better the model stability and prediction accuracy.

$$R^2 = 1 - \frac{\sum_i (\hat{y}_i - y_i)^2}{\sum_i (\bar{y}_i - y_i)^2} \tag{4}$$

$$RMSE = \sqrt{\frac{1}{m}\sum_{i=1}^{m} (y_i - \hat{y}_i)^2} \tag{5}$$

K-fold cross-validation is a common method for evaluating models, which can solve the overfitting problem [42]. Since all samples were manually collected and measured, and the total number of samples was small, the value of K was set to five. Of the samples, 80% were used for modeling, and this process was repeated five times.

3. Results

3.1. Analysis of Spectral Characteristics of Cotton Canopy at Different Disease Levels

Physiological changes caused by crop diseases affect the energy balance of crops and their interaction with solar radiation and leaves [43]. The range of 450–700 nm (visible light) constitutes a strong absorption band for leaves. Due to the strong absorption effect of photoreceptors, especially chlorophyll, a green light reflection peak at 550 nm and a red light absorption valley at 660 nm are formed, exhibiting the unique spectral characteristics of photosensitive pigments [44]. As shown in Figure 5, the spectral characteristics of cotton canopy under Fusarium wilt stress show significant differences between populations with disease indices B0, B1, B2, B3, and B4.

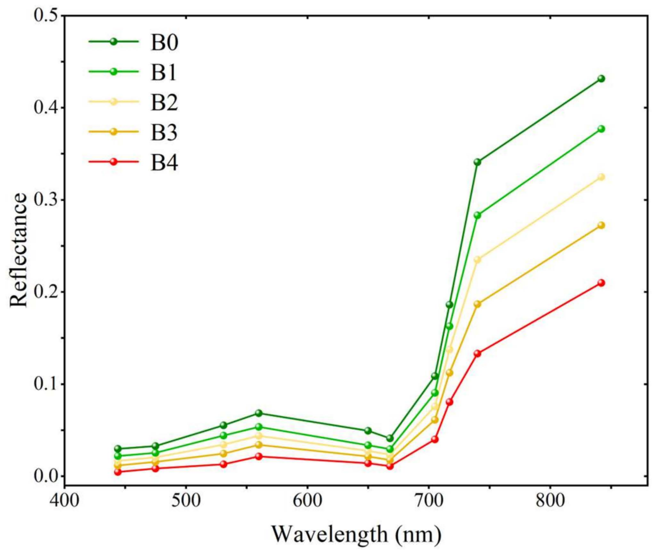

Figure 5. Spectral responses at different disease levels.

It can be observed from Figure 5 that, after cotton is infected with Fusarium wilt, the spectral characteristics undergo significant changes. With the increase in Fusarium wilt severity, its photosynthesis and chlorophyll content are affected, leading to a decreasing trend in spectral reflectance. Cotton spectral reflectance gradually increases from 444 nm to 560 nm, decreases slowly from 560 nm to 668 nm, and then gradually increases from 668 nm to 842 nm, with the highest increase rate observed at 705 nm to 740 nm. The differences in spectral characteristics of canopy between cotton plants with different severity levels of Fusarium wilt are significant. There is no significant difference in spectral reflectance between visible light and red edge (444–705 nm) ranges. However, there is a significant difference in reflectance between the red edge and near-infrared (705 nm–842 nm). The more severe the disease, the more significant the changes in the leaf reflectance characteristics of cotton, which is related to the degree of chlorophyll loss and tissue structure damage. Considering the correlation between spectral characteristics and Fusarium wilt, vegetation indices were selected as indicators for further analysis. Vegetation indices can effectively reflect the growth status and health of vegetation, closely related to the physiological changes in Fusarium wilt. Therefore, by analyzing the correlation between vegetation indices and Fusarium wilt severity indices, the mechanism of Fusarium wilt's influence on cotton vegetation spectral characteristics can be deeply understood, providing more effective methods and technical support for disease monitoring and prediction.

3.2. Data Modeling

3.2.1. Correlation Analysis

The vegetation index and the condition index were associated using the univariate linear regression model (see Figure 6). As illustrated in Figure 6, the vegetation index and the condition index all showed significant correlation, the NDWI was positively correlated with the condition index, and all other vegetation indices were negatively correlated with the condition index, indicating that the vegetation index decreased with the increase in the condition index. Since there were significant correlations between vegetation indices and condition indices, to avoid a large amount of redundancy in the data, the five vegetation indices with the highest absolute values of correlation coefficients $|r|$ (EVI, RENDVI, SAVI, MSAVI, and RDVI) were introduced as independent variables, and the condition index was used as the dependent variable, and a model was constructed to estimate the DI with PLSR and the BP neural network. Meanwhile, the model's estimation accuracy was validated by comparing the model's projected values to the measured values (R^2, $RMSE$).

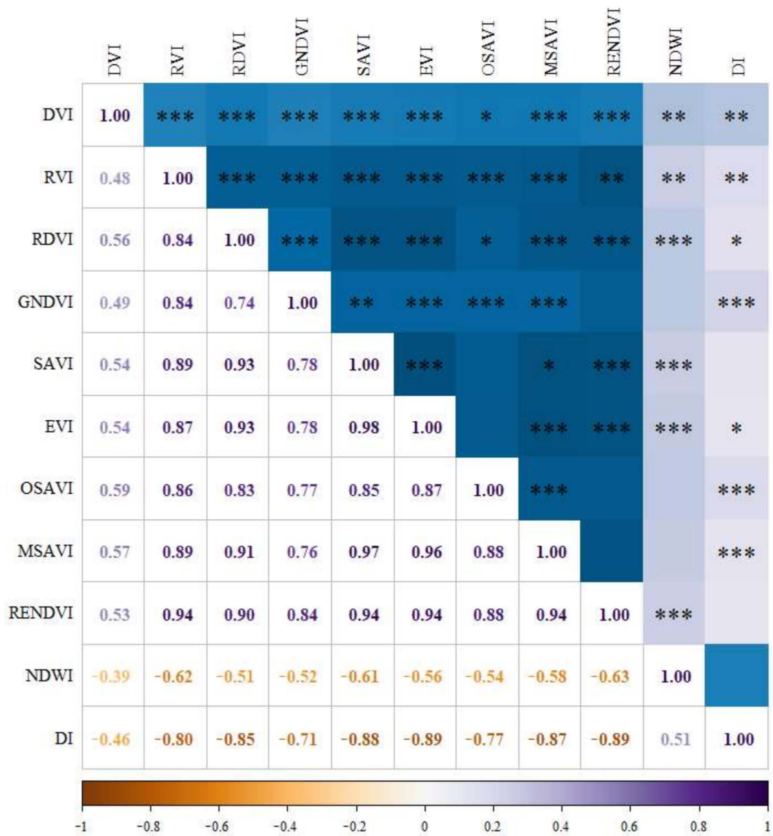

Figure 6. Correlation between several vegetation indices and the cotton Verticillium wilt disease index; *** denotes significant at the 0.001 level, ** indicates significant at the 0.01 level, and * indicates significant at the 0.05 level.

3.2.2. Partial Least Squares Regression Model

In order to compare the importance of each variable in explaining the dependent variable, the VIP values of RDVI, SAVI, EVI, MSAVI, and RENDVI were calculated, resulting in 0.968, 1.003, 1.013, 0.991, and 1.025, respectively. Among them, the VIP scores of SAVI, EVI, and RENDVI were greater than one, indicating that they all have significant effects on explaining the response variables of the model. However, the VIP values of RDVI and MSAVI were also close to one, so it is not possible to effectively determine the number of model independent variables. The study further confirmed the best variable combination using cross-validation method, based on VIP score, starting from the most important variable and adding variables one by one, and each addition was evaluated based on the model performance to determine whether the newly added variable should be retained. The cross-validation results are shown in Figure 7.

From Figure 7, it can be seen that the model performed best when selecting RENDVI and EVI as independent variables. Therefore, they were set as predictive variables for PLSR modeling of the modeling set, using the following calculation formula:

$$Y = -0.1029 \times \text{RENDVI} - 0.1108 \times \text{EVI} + 0.7318 \quad (6)$$

The test dataset was validated using the inversion model, and the accuracy of the model estimation was verified by comparing the model's estimated values with the actual measured values (R^2, $RMSE$). As shown in Figure 8, the model had good estimation accuracy on both the training set (modeling set R^2 = 0.807, $RMSE$ = 0.101) as well as the test set (test set R^2 = 0.778, $RMSE$ = 0.126), which indicates that the model can effectively predict the disease index of cotton Verticillium wilt.

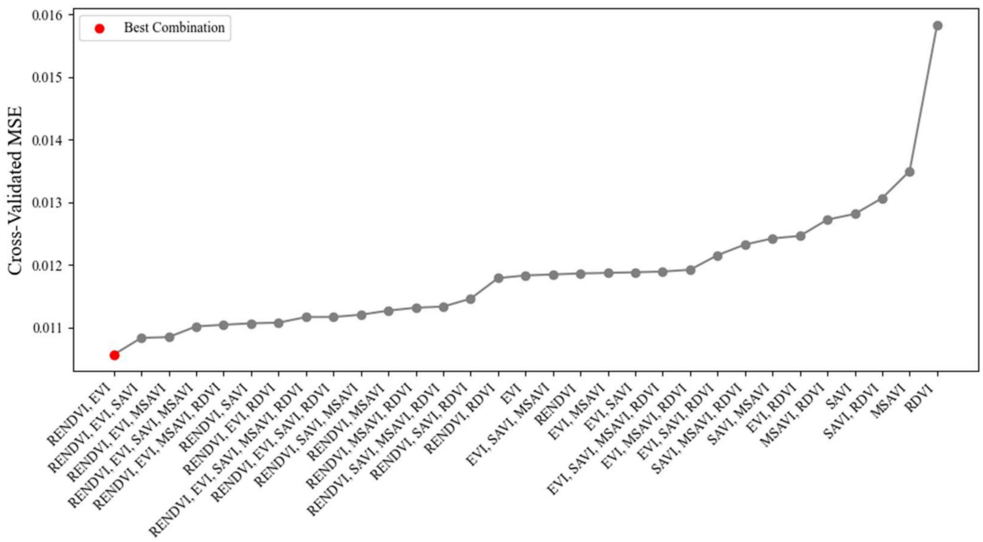

Figure 7. Cross-validated Mean Square Error for different variable combinations.

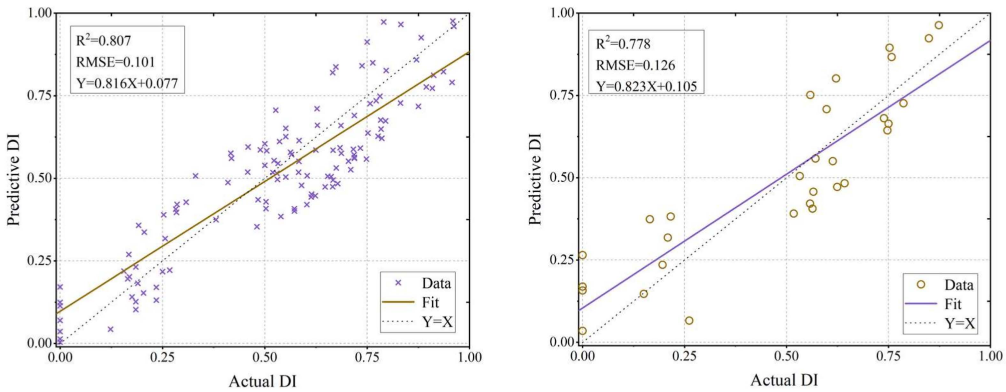

(**a**) (**b**)

Figure 8. Evaluation of the results of the PLSR model for estimating cotton DI: (**a**) evaluation of the results of the modeling set, (**b**) evaluation of the results of the testing set.

3.2.3. Backpropagation Neural Network Model

Considering that the research samples belong to a small dataset, an excessive number of hidden layers may lead to the overfitting of the model, making it unable to generalize well to new data. Therefore, this study determined the number of hidden layers as six through trial and error, and by comparing the determination coefficients of models under different neuron conditions, the number of neurons in the hidden layer was determined to be six, thus establishing the structure of the neural network. As shown in Figure 9, the vegetation index for each sample point was calculated and input it into the BP neural network for training. The input samples included EVI, RENDVI, SAVI, MSAVI, and RDVI, and the output sample was the disease index DI. Of the sample data, 80% was used for network model training, while 20% was used for model performance validation.

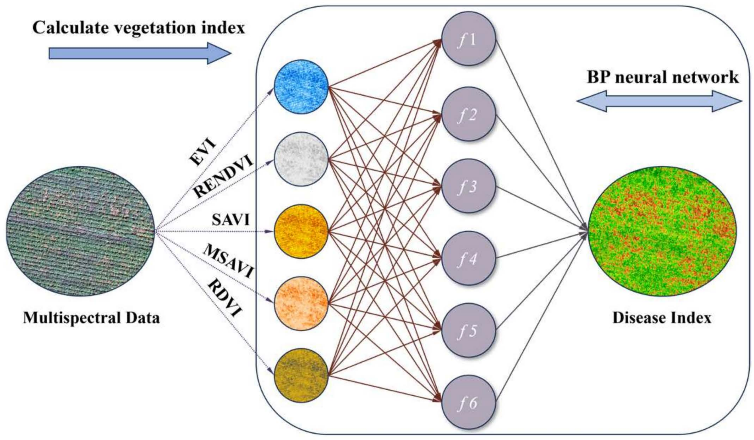

Figure 9. BP neural network model to calculate the condition index.

Figure 10 displays the model's performance on the modeling set and the test set. The model performed slightly better than PLSR on the training set, with an R^2 value of 0.846 and an $RMSE$ of 0.097, and on the test set, with an R^2 value of 0.817 and an $RMSE$ of 0.117, which can add methodological support for the prediction of the severity of Verticillium wilt disease in the test area.

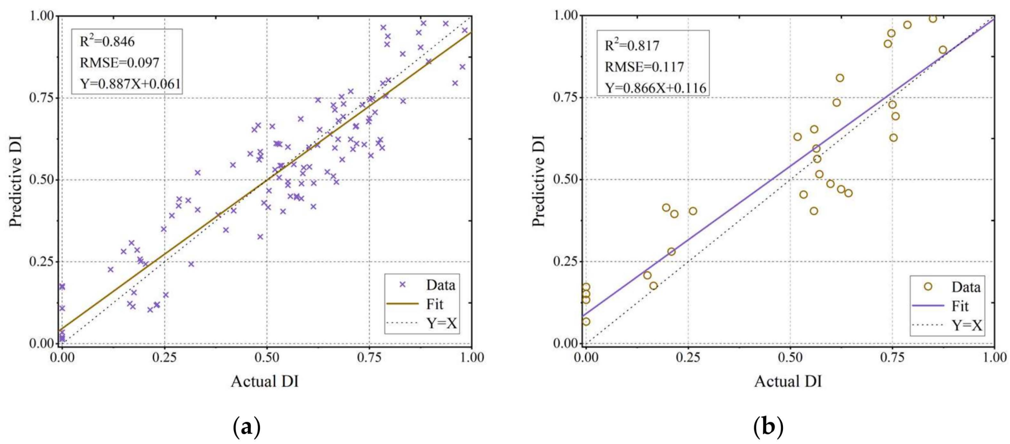

Figure 10. Evaluation of the results of the BP neural network model for estimating cotton DI: (**a**) evaluation of the results of the modeling set, (**b**) evaluation of the results of the testing set.

3.3. Cotton Verticillium Wilt Severity Assessment

The results in Section 3.2 show that both the PLSR and BP neural network models performed well on the dataset, with the BP neural network's estimation accuracy being higher than that of the PLSR. However, due to the abundance of data in the remote sensing images and in an effort to conserve computational resources, the study used the PLSR model to forecast the severity of the cotton verticillium wilt disease in the experimental field, and the results of the prediction of the Verticillium wilt disease index are shown in Figure 11. As shown in the image, the severity of cotton Verticillium wilt changes from low to high according to the color changing from yellow to red, and the figure depicts the severity of cotton Verticillium wilt in various spatial locations, which significantly reduces work intensity, expands workspace, and boosts monitoring effectiveness, when compared to the conventional manual survey.

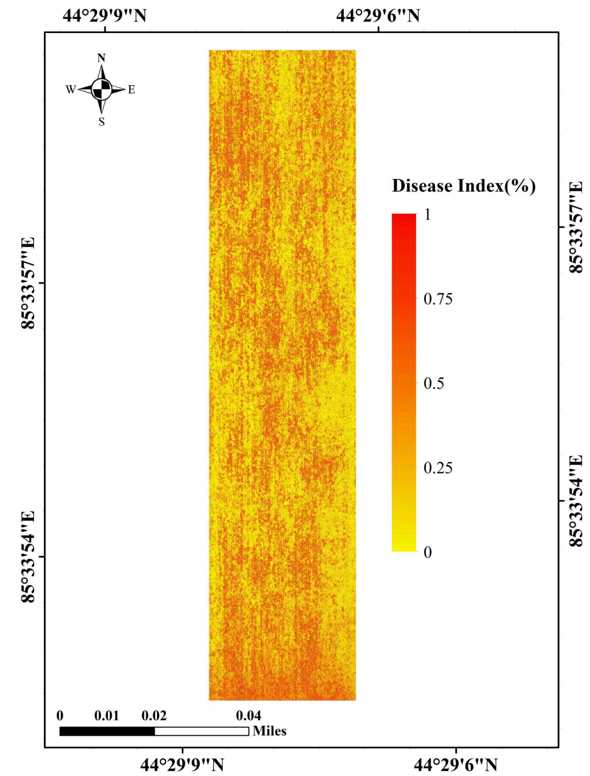

Figure 11. Predicted results of Verticillium wilt disease index.

3.4. Application Prescription Map Construction

Figure 11 displays the spatial information of the severity of cotton Verticillium wilt, showing differences in status between regions. However, it lacks information on the dosage levels of the application equipment and the geographic location of the application grid, making it unsuitable for directly guiding the application equipment to conduct spraying operations. Combining factors such as drone parameters, operational conditions, and the degree of operational quality requirements, the actual size of the prescription grid is set to 5×5 m, and spatial distribution data are resampled by the grid's mean for the division of operation areas with different pesticide application rates. The drone's unit time pesticide spraying rate can be calculated using Formula (2), ranging from 0.56–2.1 mL/min. Referring to the grading standard for Verticillium wilt and considering the response mechanism of the application equipment, the dosage of Verticillium wilt medication in cotton fields is divided into five spraying levels, corresponding to different levels of severity of Verticillium wilt. Level B0 corresponds to a spraying rate of 0; Level B1 corresponds to 0.56–0.75 mL/min; Level B2 corresponds to 0.76–1.0 mL/min; Level B3 corresponds to 1.01–1.5 mL/min; and Level B4 corresponds to 1.51–2.1 mL/min. Through the process of mining the status quo information, processing the status quo information, and mapping the presentation site, the inverse information map becomes a guidance prescription map that can be used for spraying Verticillium wilt control agents (Figure 12). The map contains high-precision geographic location information, the corresponding disease level, and the amount of pesticide applied, and the UAV sprayer can implement different pesticide spraying amounts in different spatial locations, and the prescription map can be used to guide the next stage of cotton Verticillium wilt control.

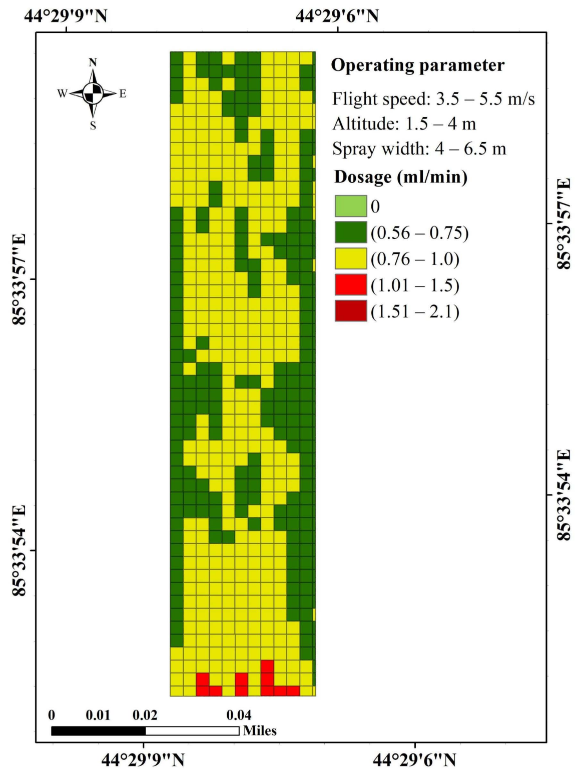

Figure 12. Prescription chart for Verticillium wilt application in cotton fields.

4. Discussion

In this study, a cotton Verticillium wilt monitoring model was constructed using high-resolution UAV multispectral images, and the model was able to swiftly and precisely assess the severity of the Verticillium wilt disease in cotton fields, and, on the basis of this, along with the agricultural UAVs' operational parameters, to assess the state of the plots where medicine was to be applied and to form a prescription map of Verticillium wilt application in cotton fields, which provides methodological references for the monitoring of cotton diseases and precise application of medicine. Compared with the traditional large-area application, this method greatly reduces the cost and improves the application efficiency. Through the analysis of cotton Verticillium wilt canopy spectra, it was found that the spectra reflectance of different severity levels had similar characteristics, with reflectance peaks near the 560 nm wavelength and absorption troughs at the 475 nm and 668 nm wavelengths. The spectral differences between different disease grades were more pronounced in the near-infrared region. Chen et al. found that the visible red light region is highly sensitive to changes in chlorophyll, which significantly decreases with increasing Verticillium wilt infection [45]. Additionally, due to the effects of leaf area index (LAI), vegetation coverage, and biomass, the canopy spectra of Verticillium wilt are more reflective than those of normal canopies. Considering the correlation between spectral features and the severity of Verticillium wilt, compared to Xavier et al. who used SVM and other classifiers to classify cotton leaf blight [12], this study directly used vegetation indices highly correlated with Verticillium wilt to invert the disease index. The study then gridded the areas to be treated, generating intuitive prescription maps, providing guidance for cotton field production management.

Traditional machine learning classification methods rely on the quality of the dataset for model accuracy. In the late stages of cotton Verticillium wilt, leaves gradually fall off, making it easy to misjudge the severity of Verticillium wilt in the area through classifiers, thus reducing the effectiveness of pesticide application. As the degree of Verticillium wilt infection increases, plants lose water, chlorophyll content decreases, and canopy disease characteristics become more pronounced, thereby enhancing the sensitivity of vegetation indices to disease response spectra. Therefore, this study combines spectral features and vegetation indices to construct PLSR and BP neural network Verticillium wilt monitoring models to spatially invert the actual severity of Verticillium wilt occurrence in cotton fields. It effectively characterizes the distribution of Verticillium wilt but cannot provide precise pesticide prescription data to drones in actual operation. Hence, this research combines factors such as the spray width of the drone sprayer, the accuracy of the positioning system, and the response speed of the spraying system, and, according to the suggestions of agronomic experts, divides the pesticide dosage for cotton Verticillium wilt into three spraying levels, generating pesticide prescription maps with geographic coordinate information to provide data support for precise pesticide application by cotton field crop protection drones.

This study constructed a cotton Verticillium wilt monitoring model and obtained a prescription map based on the inversion results. However, there are still shortcomings. Due to the limitations of manually collected data, the research data samples are relatively small. In the future, we will expand the scope of data collection to ensure that we have a diverse dataset. Additionally, we will explore methods such as using synthetic data, data augmentation techniques, and simulated data to increase the amount of data. Furthermore, in the actual field operation environment, cotton field crop protection drones face many challenges. Factors such as wind speed, terrain, and flight speed greatly interfere with achieving precise pesticide application with drones. We will conduct guided experiments on variable spraying by drones using prescription maps, while optimizing the unmanned pesticide control system to improve the deposition rate of pesticide application by drones, achieving precision spraying, and providing reliable technical means for cotton production management to increase cotton yield and quality.

5. Conclusions

This study utilized UAV to obtain high-resolution multispectral images and collected 150 sets of actual cotton Verticillium wilt data through ground surveys. Additionally, it analyzed the spectral characteristics of different disease levels in cotton canopies and calculated the correlation between different vegetation indices and cotton Verticillium wilt disease indices based on their sensitivity to spectral features. By extracting five sets of vegetation index values (EVI, RENDVI, SAVI, MSAVI, and RDVI) and calculating the cotton Verticillium wilt disease index, a cotton Verticillium wilt detection dataset was constructed, and cotton Verticillium wilt monitoring models based on PLSR and BP neural networks were developed. The detection accuracies (R^2) of the models on the modeling set were 0.807 and 0.846, and the $RMSE$ were 0.101 and 0.997, respectively. On the testing set, the detection accuracies (R^2) were 0.778 and 0.817, and the $RMSE$ were 0.126 and 0.117, respectively. The models effectively achieved cotton Verticillium wilt detection, and based on the inversion results of the model, the severity of cotton Verticillium wilt in different spatial locations was determined, reducing workload and improving monitoring efficiency. Furthermore, combined with agricultural UAV operation parameters, disease analysis was conducted on areas to be treated, forming prescription maps for cotton Verticillium wilt, providing a method reference for cotton disease monitoring and precision pesticide application.

Author Contributions: Conceptualization, Z.L. and X.L.; methodology, Z.L.; software, Z.L. and G.Y.; validation, Z.L., G.Y. and B.L.; formal analysis, Z.L.; resources, X.L.; writing—original draft preparation, Z.L.; writing—review and editing, Z.L. and X.L.; visualization, T.L.; supervision, X.L.; funding acquisition, X.L. All authors have read and agreed to the published version of the manuscript.

Funding: This work was supported in part by the National Natural Science Foundation of China under the "Research on Bionic Vision and Adaptive Grasping Methods of Xinjiang Long-staple Cotton Humanoid Picking Robot" 52265003; the Integrated Pilot Project of R&D, Manufacturing, and Application of Agricultural Machines of the Autonomous Region under the Research and Development, "Manufacturing and Application of Cotton Field Intelligent Plant Protection Equipment" 202207120037; the Autonomous Region's Tianshan Talent of Young Talented Talents of Science and

Technology under the Research on the "Visual Perception and Adaptive Control System of Humanoid Picking Robot" 600123024.

Data Availability Statement: The original contributions presented in the study are included in the article, further inquiries can be directed to the corresponding author.

Acknowledgments: We sincerely thank Tao Lin, of the Institute of Economic Crops at Xinjiang Academy of Agricultural Sciences, for his guidance and help.

Conflicts of Interest: The authors declare no conflicts of interest.

References

1. Shi, G.; Du, X.; Du, M.; Li, Q.; Tian, X.; Ren, Y.; Zhang, Y.; Wang, H. Cotton yield estimation using the remotely sensed cotton boll index from uav images. *Drones* **2022**, *6*, 254. [CrossRef]
2. Kang, X.; Huang, C.; Zhang, L.; Yang, M.; Zhang, Z.; Lyu, X. Assessing the severity of cotton verticillium wilt disease from in situ canopy images and spectra using convolutional neural networks. *Crop J.* **2023**, *11*, 933–940. [CrossRef]
3. Zhang, N.; Zhang, X.; Shang, P.; Ma, R.; Yuan, X.; Li, L.; Bai, T. Detection of cotton verticillium wilt disease severity based on hyperspectrum and gwo-svm. *Remote Sens.* **2023**, *15*, 3373. [CrossRef]
4. Azath, M.; Zekiwos, M.; Bruck, A.; Li, Y. Deep learning-based image processing for cotton leaf disease and pest diagnosis. *J. Electr. Comput. Eng.* **2021**, *2021*, 9981437.
5. Kumar, S.; Jain, A.; Shukla, A.P.; Singh, S.; Raja, R.; Rani, S.; Harshitha, G.; Alzain, M.A.; Masud, M.; Singh, D.D. A comparative analysis of machine learning algorithms for detection of organic and nonorganic cotton diseases. *Math. Probl. Eng.* **2021**, *2021*, 1790171. [CrossRef]
6. Chin, R.; Catal, C.; Kassahun, A. Plant disease detection using drones in precision agriculture. *Precis. Agric.* **2023**, *24*, 1663–1682. [CrossRef]
7. Zhang, Y.; Ma, B.; Hu, Y.; Li, C.; Li, Y. Accurate cotton diseases and pests detection in complex background based on an improved yolox model. *Comput. Electron. Agric.* **2022**, *203*, 107484. [CrossRef]
8. Dou, Z.; Fang, Z.; Han, X.; Liu, Y.; Duan, L.; Zeeshan, M.; Arshad, M. Comparison of the effects of chemical topping agent sprayed by a uav and a boom sprayer on cotton growth. *Agronomy* **2022**, *12*, 1625. [CrossRef]
9. Pergner, I.; Lippert, C. On the effects that motivate pesticide use in perspective of designing a cropping system without pesticides but with mineral fertilizer—A review. *Agron. Sustain. Dev.* **2023**, *43*, 24. [CrossRef]
10. Khan, B.A.; Nadeem, M.A.; Nawaz, H.; Amin, M.M.; Abbasi, G.H.; Nadeem, M.; Ali, M.; Ameen, M.; Javaid, M.M.; Maqbool, R.; et al. Pesticides: Impacts on agriculture productivity, environment, and management strategies. In *Emerging Contaminants and Plants: Interactions, Adaptations and Remediation Technologies*; Springer: Berlin/Heidelberg, Germany, 2023; pp. 109–134.
11. Tahir, M.N.; Lan, Y.; Zhang, Y.; Huang, W.J.; Wang, Y.; Naqvi, S.M.Z.A. Application of unmanned aerial vehicles in precision agriculture. In *Precision Agriculture*; Elsevier: Amsterdam, The Netherlands, 2023; pp. 55–70.
12. Xavier, T.W.F.; Souto, R.N.V.; Statella, T.; Galbieri, R.; Santos, E.S.; Suli, G.S.; Zeilhofer, P. Identification of ramularia leaf blight cotton disease infection levels by multispectral, multiscale uav imagery. *Drones* **2019**, *3*, 33. [CrossRef]
13. Wang, T.; Thomasson, J.A.; Yang, C.; Isakeit, T.; Nichols, R.L. Automatic classification of cotton root rot disease based on uav remote sensing. *Remote Sens.* **2020**, *12*, 1310. [CrossRef]
14. Abdalla, A.; Wheeler, T.A.; Dever, J.; Lin, Z.; Arce, J.; Guo, W. Assessing fusarium oxysporum disease severity in cotton using unmanned aerial system images and a hybrid domain adaptation deep learning time series model. *Biosyst. Eng.* **2024**, *237*, 220–231. [CrossRef]
15. Wang, C.; Chen, Y.; Xiao, Z.; Zeng, X.; Tang, S.; Lin, F.; Zhang, L.; Meng, X.; Liu, S. Cotton blight identification with ground framed canopy photo-assisted multispectral uav images. *Agronomy* **2023**, *13*, 1222. [CrossRef]
16. Lu, Z.; Huang, S.; Zhang, X.; Shi, Y.; Yang, W.; Zhu, L.; Huang, C. Intelligent identification on cotton verticillium wilt based on spectral and image feature fusion. *Plant Methods* **2023**, *19*, 75. [CrossRef] [PubMed]
17. Seol, J.; Kim, J.; Son, H.I. Field evaluations of a deep learning-based intelligent spraying robot with flow control for pear orchards. *Precis. Agric.* **2022**, *23*, 712–732. [CrossRef]
18. Storey, G.; Meng, Q.; Li, B. Leaf disease segmentation and detection in apple orchards for precise smart spraying in sustainable agriculture. *Sustainability* **2022**, *14*, 1458. [CrossRef]
19. Zanin, A.; Neves, D.C.; Teodoro, L.; Da, S.J.C.; Da, S.S.; Teodoro, P.E.; Baio, F. Reduction of pesticide application via real-time precision spraying. *Sci. Rep.* **2022**, *12*, 5638. [CrossRef] [PubMed]
20. Campos, J.; Garcia-Ruiz, F.; Gil, E. Assessment of vineyard canopy characteristics from vigour maps obtained using uav and satellite imagery. *Sensors* **2021**, *21*, 2363. [CrossRef]
21. Yu, F.; Bai, J.; Jin, Z.; Zhang, H.; Guo, Z.; Chen, C. Research on precise fertilization method of rice tillering stage based on uav hyperspectral remote sensing prescription map. *Agronomy* **2022**, *12*, 2893. [CrossRef]
22. Rudd, J.D.; Roberson, G.T. Using unmanned aircraft systems to develop variable rate prescription maps for cotton defoliants. In *2018 ASABE Annual International Meeting*; ASABE: St. Joseph, MI, USA, 2018; p. 1.

23. Li, X.; Duan, F.; Hu, M.; Hua, J.; Du, X. Weed density detection method based on a high weed pressure dataset and improved psp net. *IEEE Access* **2023**, *11*, 98244–98255. [CrossRef]
24. Chen, B.; Wang, J.; Wang, Q.; Yu, Y.; Song, Y.; Sun, L.; Han, H.; Wang, F. Yield loss estimation of verticillium wilt cotton field based on uav multi-spectral and regression model. In Proceedings of the 2022 Global Conference on Robotics, Artificial Intelligence and Information Technology (GCRAIT), Chicago, IL, USA, 30–31 July 2022.
25. Qiao, L.; Tang, W.; Gao, D.; Zhao, R.; An, L.; Li, M.; Sun, H.; Song, D. Uav-based chlorophyll content estimation by evaluating vegetation index responses under different crop coverages. *Comput. Electron. Agric.* **2022**, *196*, 106775. [CrossRef]
26. Aldubai, A.A.; Alsadon, A.A.; Al-Gaadi, K.A.; Tola, E.; Ibrahim, A.A. Utilizing spectral vegetation indices for yield assessment of tomato genotypes grown in arid conditions. *Saudi J. Biol. Sci.* **2022**, *29*, 2506–2513. [CrossRef] [PubMed]
27. Radócz, L.; Szabó, A.; Tamás, A.; Illés, Á.; Bojtor, C.; Ragán, P.; Vad, A.; Széles, A.; Harsányi, E.; Radócz, L. Investigation of the detectability of corn smut fungus (ustilago maydis dc. Corda) infection based on uav multispectral technology. *Agronomy* **2023**, *13*, 1499. [CrossRef]
28. Shahi, T.B.; Xu, C.; Neupane, A.; Guo, W. Recent advances in crop disease detection using uav and deep learning techniques. *Remote Sens.* **2023**, *15*, 2450. [CrossRef]
29. Jordan, C.F. Derivation of leaf-area index from quality of light on the forest floor. *Ecology* **1969**, *50*, 663–666. [CrossRef]
30. Zhao, H.; Yang, Y.; Yang, C.; Song, R.; Guo, W. Evaluation of spatial resolution on crop disease detection based on multiscale images and category variance ratio. *Comput. Electron. Agric.* **2023**, *207*, 107743. [CrossRef]
31. Gao, C.; Ji, X.; He, Q.; Gong, Z.; Sun, H.; Wen, T.; Guo, W. Monitoring of wheat fusarium head blight on spectral and textural analysis of uav multispectral imagery. *Agriculture* **2023**, *13*, 293. [CrossRef]
32. Jiang, P.; Zhou, X.; Liu, T.; Guo, X.; Ma, D.; Zhang, C.; Li, Y.; Liu, S. Prediction dynamics in cotton aphid using unmanned aerial vehicle multispectral images and vegetation indices. *IEEE Access* **2023**, *11*, 5908–5918. [CrossRef]
33. Lizarazo, I.; Rodriguez, J.L.; Cristancho, O.; Olaya, F.; Duarte, M.; Prieto, F. Identification of symptoms related to potato verticillium wilt from uav-based multispectral imagery using an ensemble of gradient boosting machines. *Smart Agric. Technol.* **2023**, *3*, 100138. [CrossRef]
34. Nguyen, C.; Sagan, V.; Skobalski, J.; Severo, J.I. Early detection of wheat yellow rust disease and its impact on terminal yield with multi-spectral uav-imagery. *Remote Sens.* **2023**, *15*, 3301. [CrossRef]
35. Zhang, R.; Hewitt, A.J.; Chen, L.; Li, L.; Tang, Q. Challenges and opportunities of unmanned aerial vehicles as a new tool for crop pest control. *Pest Manag. Sci.* **2023**, *79*, 4123–4131. [CrossRef]
36. Shu, M.; Bai, K.; Meng, L.; Yang, X.; Li, B.; Ma, Y. Assessing maize lodging severity using multitemporal uav-based digital images. *Eur. J. Agron.* **2023**, *144*, 126754. [CrossRef]
37. Yu, T.; Zhou, J.; Fan, J.; Wang, Y.; Zhang, Z. Potato leaf area index estimation using multi-sensor unmanned aerial vehicle (uav) imagery and machine learning. *Remote Sens.* **2023**, *15*, 4108. [CrossRef]
38. Sahoo, R.N.; Rejith, R.G.; Gakhar, S.; Ranjan, R.; Meena, M.C.; Dey, A.; Mukherjee, J.; Dhakar, R.; Meena, A.; Daas, A.; et al. Drone remote sensing of wheat n using hyperspectral sensor and machine learning. *Precis. Agric.* **2024**, *25*, 704–728. [CrossRef]
39. Yin, C.; Lv, X.; Zhang, L.; Ma, L.; Wang, H.; Zhang, L.; Zhang, Z. Hyperspectral uav images at different altitudes for monitoring the leaf nitrogen content in cotton crops. *Remote Sens.* **2022**, *14*, 2576. [CrossRef]
40. Rumelhart, D.E.; Hinton, G.E.; Williams, R.J. Learning representations by back-propagating errors. *Nature* **1986**, *323*, 533–536. [CrossRef]
41. Xu, W.; Chen, P.; Zhan, Y.; Chen, S.; Zhang, L.; Lan, Y. Cotton yield estimation model based on machine learning using time series uav remote sensing data. *Int. J. Appl. Earth Obs.* **2021**, *104*, 102511. [CrossRef]
42. Siegfried, J.; Adams, C.B.; Rajan, N.; Hague, S.; Schnell, R.; Hardin, R. Combining a cotton 'boll area index' with in-season unmanned aerial multispectral and thermal imagery for yield estimation. *Field Crop. Res.* **2023**, *291*, 108765. [CrossRef]
43. Farella, M.M.; Fisher, J.B.; Jiao, W.; Key, K.B.; Barnes, M.L. Thermal remote sensing for plant ecology from leaf to globe. *J. Ecol.* **2022**, *110*, 1996–2014. [CrossRef]
44. Zhen, S.; Kusuma, P.; Bugbee, B. Chapter 17-toward an optimal spectrum for photosynthesis and plant morphology in led-based crop cultivation. In *Plant Factory Basics, Applications and Advances*; Kozai, T., Niu, G., Masabni, J., Eds.; Academic Press: Cambridge, MA, USA, 2022; pp. 309–327.
45. Chen, B.; Wang, K.; Li, S.; Wang, J.; Bai, J.; Xiao, C.; Lai, J. Spectrum Characteristics of Cotton Canopy Infected with Verticillium wilt and Inversion of Severity Level. Li, D., Ed.; Springer: Boston, MA, USA, 2008.